Proxima Centauri b: infrared detectability in presence of stellar activity

Proxima Centauri b: infrared detectability in presence of stellar activity

D Galuzzo, F Berrilli, and L Giovannelli

Università degli Studi di Roma "Tor Vergata", Via della Ricerca Scientifica 1, 00133 Rome, Italy

E-mail: daniele.galuzzo@roma2.infn.it

Abstract. We propose a general method to detect and characterize tidally-locked exoplanets in 1:1 spin/orbit resonance using the information coming from different infrared bands, analyzing the variation in time of the color of exoplanetary systems. We focus on the effects induced on the detectability of the system by the starspots of the active host-stars. The analysis is conducted on the Proxima Centauri system as a case study, comparing the results from a more complex 3D General Circulation Model simulation with a simple toy model. Our toy model includes the black-body emission in the infrared of the host-star, day-side and night-side of the tidally locked planet, as well as the starspots. The results are consistent with the 3D General Circulation Model and suggests that it is possible to disentangle the stellar activity effects from the presence of the planet in the exoplanetary system using the infrared color-color diagram technique.

1. Introduction

The number of known exoplanets is increasing with time [1] thanks to a number of ground-based and space-dedicated missions developed in the last years. Detection methods include radial velocity, transit, direct imaging and microlensing, but most of these exoplanets are found with the transit method [1]. This method requires the alignment of the planet orbital plane with the host-star disk, along the observer's line of sight in order to observe the star light dim due to the transit of the planet. However, just analyzing the geometric probability of a planet transit in front of a star, that is $P_{tr} = R_{star}/a$, where R_{star} is the star radius and a is the semi-major axis of the planet's orbit, it is clear that only a small fraction of all planets appear to be transiting. Moreover, observational biases are introduced by observing transiting planets [2]. For example, the detection of planets closer to their host-stars is facilitated. In addition, the more a planet is close to the star, the more is the probability that it is captured in gravitational spin/orbit resonances. Of particular scientific interest are those planets that could be captured in 1:1 spin/orbit resonance, i.e. that are locked to face the host-star always with the same hemisphere.

A possible detection strategy to extract information about atmosphere and climate of a planet is to analyze its thermal emission [3]. Typically, the peak of emission of a planet in the host-star habitable zone is expected to be in the mid-IR region, i.e. between $5 \div 20\,\mu$m, depending on its temperature. However, most of the times, the direct detection of planetary thermal emission is

[1] https://exoplanetarchive.ipac.caltech.edu/exoplanetplots/

quite challenging, since the host-star emission at all wavelengths is usually order of magnitudes larger compared to that of planets.

A way to identify planets with dense atmospheres was suggested by [4] and consists in the analysis of the broadband mid-IR flux variations observed in a planet/star system due to the orbital phase of the planet. This flux variation, also known as thermal phase curve, is larger when the considered host-star is a red dwarf, since the radius of the star is smaller and the contribution of the planet is greater. In that case, the planet/star flux ratio in the mid-IR could reach $10^{-6} \div 10^{-4}$ and it could be detected by current telescopes. This is one of the reasons why the M-type main sequence stars are commonly believed to be prime targets for the search of exoplanets. Moreover, M-dwarf stars are also the most abundant and long-lived stars in the Milky Way. On the other hand, these stars show a huge short term variability, being very active with a high rate of powerful flares [5, 6] which can significantly modify the spectral flux of the star. These events, related to the star magnetic activity, could be associated with the formation of big starspots on the photosphere, because of the convective nature of the M-type stars [7].

In this work, we propose an indirect exoplanet detection method based on the color variation of a planetary system due to the different planet contributions during its orbit. With this method we are also able to detect features on the star photosphere and understand how to disentangle the effects of the presence of an exoplanet from the effects of an active host-star. Furthermore, our method does not require a transiting planet, but can be applied also to non-transiting ones. It can also be applied together with other methods in order to confirm a detection or to extract complementary or missing data. The technique was developed in [8] and is focused on the broadband infrared (IR) emission of the exoplanetary system, assuming the detection of the combined flux of the host-star and exoplanet IR emission. The technique takes advantage of using the variations of color in time, defining the color indexes in the IR standard bands M, N and Q_0. The use of color indexes focus the attention on the change of steepness of the star/planet combined spectrum, reducing spurious effects due to the overall flux variation (see e.g. the use of the color index in [9]).
To evaluate the fluxes in the mentioned bands, we developed a toy model which calculates the black-body radiation, starting from the planet surface temperature and the star photosphere temperature. The surface and photosphere temperature patterns are based on the results found in literature for the Proxima Centauri planetary system. To build the planet surface temperature field, we refer to [10], [11] and [12], analyzing the case of a tidally-locked planet (i.e. 1:1 spin/orbit resonance). For the properties and characteristics of Proxima Centauri (i.e. photosphere temperature, rotation period and starspot temperature) we refer to [13] and [14].

2. Simulation and results

In this work we use a simplified approach to test if the IR color-color technique is able to disentangle the effects of the presence of an exoplanet from the effects of an active host-star. As a case study we take in consideration the Proxima Centauri system, described in [8], where a more detailed simulation and analysis was performed using the PLASIM 3D General Circulation Model (GCM).

In this case, we schematize the host-star as a spherical black-body emitter, with an effective temperature $T_{star} = 3000$ K. The starspot covers an area equal to the 0.05% of the entire star surface, with a temperature set to $T_{spot} = 2800$ K. The starspot is in solid rotation with the star, with a period of 78 days, as discussed in [14]. In the left panel of Fig. 1 we show the Spectral Energy Distribution (SED) of the Sun and Proxima Centauri, compared with the relative black-body radiation curves, as a function of wavelength. The effective temperature used to obtain the curve relative to the Sun is $T_{sun} = 6000$ K. On the right panel of Fig. 1, the comparison between the Proxima Centauri SED and black-body emission with the planet

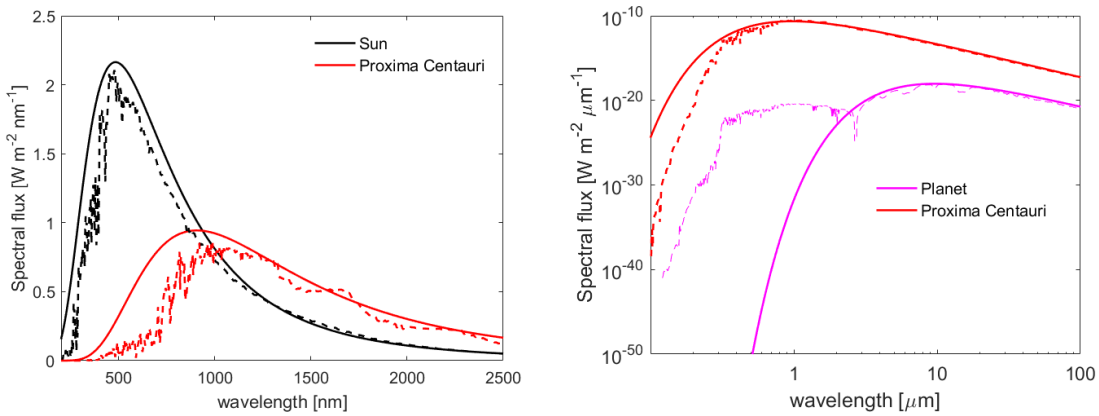

Figure 1. On the left: comparison between observed spectral flux of the Sun and Proxima Centauri (dashed black and red line, respectively) and the black-body at their effective temperature (solid line). The fluxes are computed at the top of the atmosphere of the Earth and Proxima b respectively. On the right comparison between observed spectral flux of Proxima Centauri (dashed red line) and simulated spectal flux with the radiative transfer model *uvspec* using the output from the PLASIM 3D atmospheric model for the exoplanet Proxima b (dashed purple line). All quantities are computed at Earth distance from Proxima Centauri system. Solid lines represents, respectively, the effective temperature for the star (solid red) and the spectrum of the black-body at the temperature of the sub-stellar point of the planet (solid purple).

emission is shown on a log-log scale. In particular, the purple dashed curve is the composition of the reflected (below 3 μm) and emitted (above 3 μm) radiation by the planet, whereas the purple solid curve represents the planet IR black-body radiation, without any reflection. It is clear how above 10 μm, the difference between the star and planet emissions is sufficiently small to allow the detection of a flux variation due to the planet orbital phase. Furthermore, in that spectral region, the black-body curve is a quite good approximation for both planet and star emissions.

The exoplanet is schematized as a spherical body in 1:1 spin/orbit resonance with the star, characterized by a surface temperature at the sub-stellar point $T_{sub} = 300$ K, a surface temperature at the anti-stellar point of $T_{anti} = 125$ K, and a constant meridional and zonal temperature gradient along the surface. The planet has an orbital period of 11.186 days. In this case study, we fixed the orbital inclination of the system with respect to the observer to be 90° (i.e. as for a transiting planet), to simulate the maximum possible effect. For simplicity we neglect the effects of the transit in the photometry, thus providing the information on the efficiency of the technique for non-transiting exoplanets at the best conditions.

We consider three different cases for our computations (see also Fig. 2).

- **CASE 1** host-star, no starposts and the exoplanet. This case is our reference case with respect to the analysis performed with the 3D GCM in [8].
- **CASE 2** host-star with one starspot, no exoplanet. This case is used to analyze the effect of the sole star activity.
- **CASE 3** host-star with one starspot and the exoplanet. This cased is used to test the performance of the technique in distinguishing star activity from the effects of the exoplanet presence.

We compute in these three cases the flux from the planet and from the star in the IR broadbands of interest. Thermal phase curves are computed using the F2550W band of the

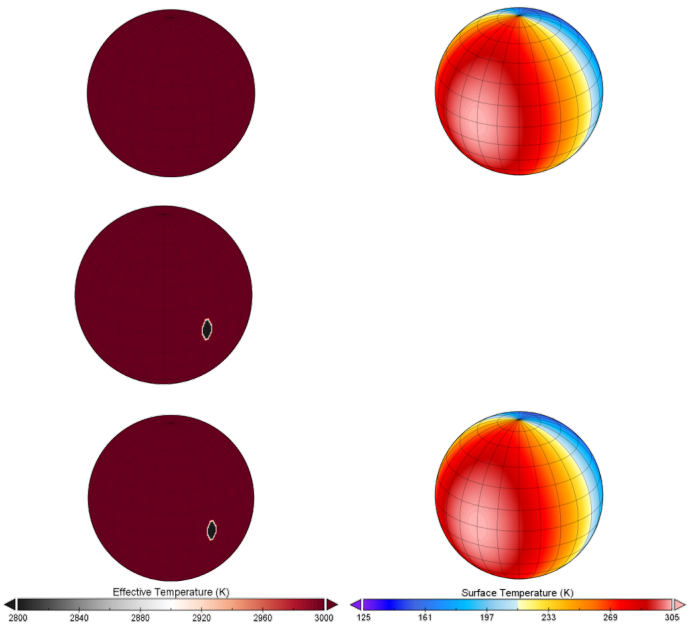

Figure 2. Schematic representation of the emitting sources in three simulations. Top row, CASE 1, host-star (no starspots) and exoplanet. Middle row, CASE 2, host-star with starspot, no exoplanet. Bottom row, CASE 3, host-star with starspot and exoplanet.

MIRI instrument on board of the James Webb Space Telescope (23.5 μm $\div$ 27.5 μm). The relative photometric error band is computed assuming photon noise limited observations.

The IR color-color technique is defined on the magnitude of the combined planet and star emission in the three cases in the standard bands M, N and Q_0. We define the color variation as

$$\Delta(X-Y) = (X-Y) - \overline{(X-Y)}, \tag{1}$$

where X and Y for one color is M and N, while for the other color is N and Q_0. $\overline{X-Y}$ is the mean over the orbital period.

In Fig. 3 the results of the computations are shown. In the first row we show the results from the 3D GCM simulation, to be compared with the second row, where similar parameters were used in our simplified approach. For the cases 1-3, we consider a full rotation of the star to compute the contribution of the starspot. This gives us a different time span of the simulation compared to the PLASIM case. Nevertheless, data is often overlapped, showing only the final orbit. This is the case for the first two color-color diagrams in Fig. 3. The amplitude of the thermal phase curve in the two cases is in good agreement, as it is also for the extension of the scatterplot in the color-color diagram. This suggests that the computation based on the black-body emission, although simplified, catches the basic physical properties of the exoplanetary system and can be used to study observational parameters of the system. The color-color diagram is more linear in the case of the PLASIM simulation; this behavior could be due to the planet surface temperature pattern and can be further investigated in future simulations. In the third row we show the case of the star with a single starspot corotating with the same rotation period of the star. The thermal phase curve, in the absence of the exoplanet, is substituted with the flux from the star in the same band (F2550W) as a function of time. As expected, the color-color diagram shows a variation in the portion of the orbital period, when the starspot is visible from the observer.

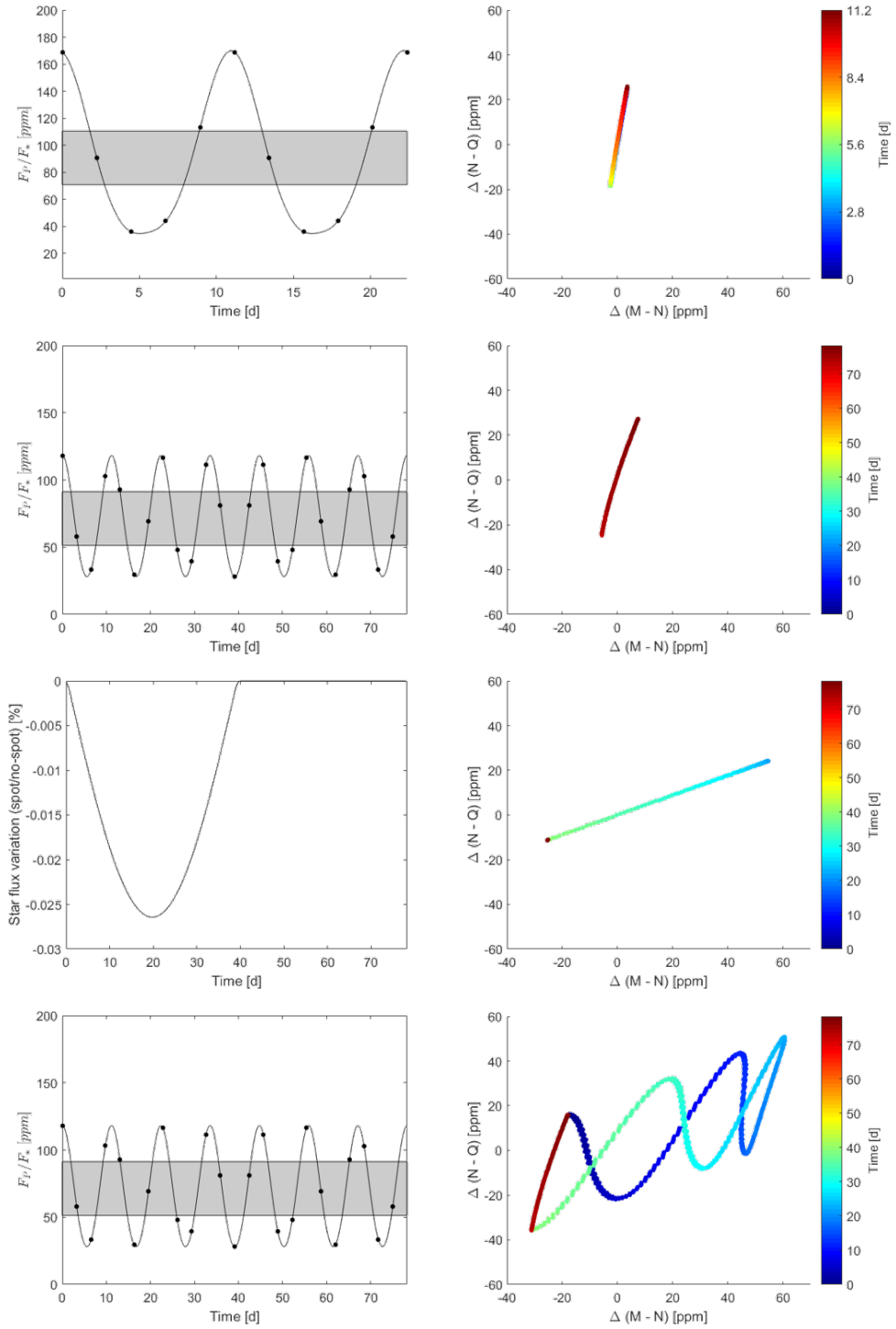

Figure 3. Results from the simulations. On the left column we show the thermal phase curves of the exoplanetary system, as a function of time in days, except on the third row where there is no exoplanet. In this case, we show the flux variation due to the presence of the starspot. On the right column, we show the color-color variation scatterplots. The colorbars represent the time in days along the orbit. From the top to the bottom, data refers to: GCM simulation with PLASIM, CASE 1, CASE 2 and CASE 3 of our computations with black-body emission.

Interestingly, the variation in the color-color space has a different slope with respect to the case of the presence of the sole exoplanet: 0.4 instead of 3.9. The magnitude of the effect in the color variation is instead slightly greater with respect to the exoplanet case. This is further confirmed in the fourth row where the two effects are combined. In the first half rotation of the star ($\sim$ 39 days), the presence of the starspot spread out the color variation along the same direction showed in the CASE 2, making also possible to distinguish the effects of the exoplanet on 3.5 planet orbital periods. In the second half of the simulation the starspot is not visible and the patter is the same as in CASE 1, apart from an offset. Note that no visible effect is produced on the thermal phase curve with respect to the CASE 1, since the stellar flux variation due to the starspot is of the order of 10^{-5}, while the planet flux variation is of the order 10^{-4}. The IR color-color technique instead can be used to disentangle the two effects since the spread in the 2D space occurs in different directions.

3. Conclusion

We have presented a simplified computation for the detectability of exoplanetary system using the IR color-color technique in the presence of stellar activity. As shown, the IR color-color technique can be used to disentangle the effect of an exoplanet from the stellar activity effects. The Principal Component Analysis (PCA) could be used to project the data in an appropriate 2D space where the effects of the exoplanet and the starspot are orthogonal. This could boost the possibility to detect exoplanets, also in presence of stellar activity.

Furthermore this toy model can be used to easily explore the parameter space, to investigate the slope in the color-color space as a function of the effective temperature of the star, the starspot and the planet surface temperature pattern. The stellar activity can be also further explored, varying the number of starspots, their latitude, extension and temperature as well as the presence of faculae and the rotation properties (differential rotation) and their variations with the stellar magnetic cycle.

References

[1] Koch D G, Borucki W J, Webster L, Dunham E W, Jenkins J M, Marriott J and Reitsema H J 1998 Kepler: a space mission to detect earth-class exoplanets
[2] M Kipping D and Sandford E 2016 *MNRAS* **463** stw1926
[3] Kreidberg L and Loeb A 2016 *ApJ* **832** L12
[4] Selsis F 2004 *Extrasolar Planets: Today and Tomorrow* (*Astronomical Society of the Pacific Conference Series* vol 321) ed Beaulieu J, Lecavelier Des Etangs A and Terquem C p 170
[5] Howard W S *et al.* 2018 *ApJ* **860** L30
[6] Sparks W B, White R L, Lupu R E and Ford H C 2018 *ApJ* **854** 134
[7] Barnes J R, Jeffers S V, Jones H R A, Pavlenko Y V, Jenkins J S, Haswell C A and Lohr M E 2015 *ApJ* **812** 42
[8] Galuzzo D, Berrilli F, Cagnazzo C, Fierli F and Giovannelli L 2019 *ApJ* submitted
[9] Lovric M, Tosone F, Pietropaolo E, Moro D D, Giovannelli L, Cagnazzo C and Berrilli F 2017 *J. Space Weather Space Clim.* **7** A6
[10] Turbet M, Leconte J, Selsis F, Bolmont E, Forget F, Ribas I, Raymond S N and Anglada-Escudé G 2016 *A&A* **596**
[11] Boutle I A, Mayne N J, Drummond B, Manners J, Goyal J, Lambert F H, Acreman D M, and Earnshaw P D 2017 *A&A* **601**
[12] Del Genio A D, Way M J, Amundsen D S, Aleinov I, Kelley M, Kiang N Y and Clune T L 2019 *Astrobiology*
[13] Ribas I, Gregg M D, Boyajian T S and Bolmont E 2017 *A&A* **603** A58
[14] Berdyugina S V 2005 *Living Reviews in Solar Physics* **2** 8 ISSN 1614-4961